



HAL
open science

Effects of laser wavelength and density scalelength on absorption of ultrashort intense lasers on solid-density targets

Susumu Kato, Eiichi Takahashi, Tatsuya Aota, Yuji Matsumoto, Isao Okuda,
Yoshiro Owadano

► **To cite this version:**

Susumu Kato, Eiichi Takahashi, Tatsuya Aota, Yuji Matsumoto, Isao Okuda, et al.. Effects of laser wavelength and density scalelength on absorption of ultrashort intense lasers on solid-density targets. 2004. hal-00001970

HAL Id: hal-00001970

<https://hal.science/hal-00001970>

Preprint submitted on 23 Oct 2004

HAL is a multi-disciplinary open access archive for the deposit and dissemination of scientific research documents, whether they are published or not. The documents may come from teaching and research institutions in France or abroad, or from public or private research centers.

L'archive ouverte pluridisciplinaire **HAL**, est destinée au dépôt et à la diffusion de documents scientifiques de niveau recherche, publiés ou non, émanant des établissements d'enseignement et de recherche français ou étrangers, des laboratoires publics ou privés.

Effects of Laser Wavelength and Density Scalelength on Absorption of Ultrashort Intense Lasers on Solid-Density Targets

Susumu Kato[§], Eiichi Takahashi, Tatsuya Aota,
Yuji Matsumoto, Isao Okuda, and Yoshiro Owadano

National Institute of Advanced Industrial Science and Technology (AIST), Tsukuba,
Ibaraki 305-8568, Japan

Abstract. Hot electron temperatures and electron energy spectra in the course of interaction between intense laser pulse and overdense plasmas are reexamined from a viewpoint of the difference in laser wavelength. The hot electron temperature measured by a particle-in-cell simulation is scaled by I rather than $I\lambda^2$ at the interaction with overdense plasmas with fixed ions, where I and λ are the laser intensity and wavelength, respectively.

1. Introduction

The interaction of intense laser pulses with overdense plasmas has attracted much interest for the fast ignitor concept in inertial fusion energy [1]. The interaction of ultrashort intense laser pulses with thin solid targets have also been of great interest for the application to high energy ion sources [2]. Ultraintense irradiation experiments using an infrared subpicosecond laser, e.g., Nd:glass ($\lambda = 1,053$ nm) or Ti:sapphire ($\lambda = 800$ nm) lasers, whose powers and focused intensities exceed 100 TW and 10^{20} W/cm², are possible using chirped pulse amplification techniques [3]. In these experiments, the classical normalized momentum of electrons $a_0 \equiv P_{osc}/mc = (I\lambda_\mu^2/1.37 \times 10^{18})^{1/2} \geq 1$, where m is the electron mass, c is the speed of light, I is the laser intensity in W/cm², and λ_μ is the wavelength in μm . On the other hand, a KrF laser ($\lambda = 248$ nm) has an advantage as the fast ignitor in that the critical density is close to the core, and hot electron energies are suitable since the critical density of the KrF laser is ten times greater than that of an infrared laser [4]. The peak intensities of KrF laser systems were only the order of 10^{18} W/cm², namely $a_0 < 1$ [5]. Therefore, the dependence of the laser plasma interactions on the laser wavelength was not investigated in $a_0 \geq 1$. Recently, the laser absorption and hot electron generation have been studied by the high intensity KrF laser system of which focused intensity is greater than 10^{19} W/cm² [6]. However, the production of hot electrons by the high intensity KrF laser has not been

[§] (s.kato@aist.go.jp)

fully understood yet. Namely, it has been not clear that the effects of laser wavelength on hot electrons produced by ultrashort intense laser pulse on solid-density targets.

The absorption, electron energy spectrum, and hot electron temperature have usually been investigated and scaled using the parameters $I\lambda^2$, n_e/n_c , and L/λ [7, 8], where n_e , n_c , and L are the electron density, critical density, and density scale length, respectively. Critical density absorption of the laser light converts laser energy into hot electrons having a suprathermal temperature T_h approximately proportional to $\sqrt{I\lambda^2}$ for $a_0 > 1$, and $T_h \sim [(1 + a_0^2)^{1/2} - 1]mc^2$ at moderate densities [9], where $mc^2 = 511$ keV, m is an electron rest mass. The scaling of the hot electron temperature has been supported by experiments of Nd:glass and Ti:sapphire lasers [10]. On the other hand, the results of one-dimensional simulation for normal incidence in the density region $4 < n_e/n_c < 100$ and the normalized intensity $4 < a_0^2 < 30$ have shown that $T_h \sim \eta (n_e/n_c)^\alpha [(1 + a_s^2)^{1/2} - 1]mc^2$, where $a_s = \beta a_0 (n_c/n_e)^{1/2}$ is the electromagnetic fields at the surface of the overdense plasma, $\eta = 0.5 \sim 1.1$ and $\alpha = 1/2$, which depend weakly on $I\lambda^2$ and n_e/n_c [8]. β is weakly depend on the angle of incidence, absorption rate, and n_{e0}/n_c [11]. The hot electron temperature is scaled by the amplitude of electromagnetic fields at the plasma surface rather than that in vacuum; namely, the hot electron temperature is slightly dependent on the wavelength.

In addition, at the interaction of intense laser pulses with solid density plasma which has a sharp density gradient the hot electron temperature is scaled by $I\lambda^{-1}$ rather than $I\lambda^2$ [12]. In the present paper, we study the absorption of ultrashort intense laser pulses on overdense plasmas for different laser wavelengths ($\lambda = 0.25, 0.5$, and $1 \mu\text{m}$) using a particle-in-cell (PIC) simulation.

2. PIC simulation

In order to investigate hot electron generation for oblique incidence, we use the relativistic 1 and 2/2 dimensional PIC simulation with the boost frame moving with $c \sin \theta$ parallel to the target surface, where c and θ are the speed of light and an angle of incidence [13]. In the simulation, the target is the fully ionized plastic and the electron density $n_{e0} \sim 3.5 \times 10^{23} \text{cm}^{-3}$. The density correspond to $n_{e0}/n_c = 20, 78$, and 310 for $\lambda = 0.25, 0.5$, and $\lambda = 1 \mu\text{m}$, respectively. The density profile has a sharp density gradient, $n_e(x) = n_{e0}$ for $x \geq 0$ and $n_e(x) = 0$ for $x < 0$. In order to clarify the boundary effect, ions are fixed, namely, the boundary does not move all the time. The laser pulse starts at $x < 0$ and propagates towards $x > 0$. The laser intensity rises in 5 fs and remains constant after that. The irradiated intensity $I = 5 \times 10^{19} \text{W/cm}^2$ and the angle of incidence $\theta = 30^\circ$ and 45° (p-polarized), respectively. $a_0^2 = 2.3, 9.2$, and 36 for $\lambda = 0.25, 0.5$, and $1.0 \mu\text{m}$, respectively. However, $a_s^2 = 0.12\beta$ for all wavelength. Normalized electron energy distributions after 50 fs are shown in Fig.1(a) and 1(b) for $\theta = 30^\circ$ and 45° , respectively. The hot electron temperatures are 140 and 340 keV for $\theta = 30^\circ$ and 45° , respectively. The hot electron temperatures does not depend on the laser wavelength. The result is well agreement with that of a simple sharp boundary theory.

On the other hand, the absorption depends on the laser wavelength, $A(\theta = 30^\circ) = 0.9\text{-}1.8\%$, $2.2\text{-}3.0\%$, and $3.6\text{-}4.3\%$ and $A(\theta = 45^\circ) = 2.6\text{-}4.1\%$, $5.3\text{-}6.7\%$, and $7.8\text{-}9.0\%$ for $\lambda = 1.0, 0.5,$ and $0.25 \mu\text{m}$, respectively.

3. Concluding Remarks

The effects of laser wavelength on hot electrons produced by ultrashort intense laser pulse on solid-density targets are studied by the use of a PIC simulation. As a result, the dependence to the wavelength of hot electron temperature strongly depend on the boundary condition, even in the one dimensional case, namely, all are not determined only by $I\lambda^2$. The density profiles of both preformed plasma [16] and multi-dimensional effects such as surface deformation [9] are very important in the actual experiments.

Acknowledgments

A part of this study was financially supported by the Budget for Nuclear Research of the Ministry of Education, Culture, Sports, Science and Technology, based on the screening and counseling by the Atomic Energy Commission.

References

- [1] M. Tabak *et al.*, Phys. Plasmas **1**, 1626 (1994); R. Kodama *et al.*, Nature **412**, 798 (2001).
- [2] D. Umstadter, J. Phys. D **36** R151 (2003); S. P. Hatchett *et al.*, Phys. Plasmas **7**, 2076 (2000),
- [3] P. Maine *et al.*, IEEE J. Quantum Electron. **24**, 398 (1988); M. D. Perry *et al.*, Opt. Lett. **24**, 160 (1999).
- [4] M. J. Shaw *et al.*, Fusion Eng. Des. **44**, 209 (1999).
- [5] U. Teubner *et al.*, Phys. Rev. E **54**, 4167 (1996); M. Borghesi *et al.*, Phys. Rev. E **60**, 7374 (1999).
- [6] E. Takahashi *et al.*, *Proceedings of the Third International Conference on Inertial Fusion Sciences and Applications (IFSA2003)*, Editors: B. A. Hammel D. D. Meyerhofer J. Meyer-ter-Vehn H. Azechi, p.406 (American Nuclear Society, Inc., 2004).
- [7] E. Lefebvre and G. Bonnaud, Phys. Rev. E **55**, 1011 (1997).
- [8] S. C. Wilks and W. L. Kruer, IEEE J. Quantum Electron. **33**, 1954 (1997)
- [9] S. C. Wilks, Phys. Fluids B **5**, 2603 (1993); S. C. Wilks *et al.*, Phys. Rev. Lett. **69**, 1383 (1992).
- [10] G. Malka and J. L. Miquel, Phys. Rev. Lett. **77**, 75 (1996); Y. Oishi *et al.*, Appl. Phys. Lett. **79**, 1234 (2001).
- [11] A. Lichters *et al.*, Phys. Plasmas **3**, 3425 (1996)
- [12] S. Kato *et al.*, J. Plasma Fusion Res. **78**, 717 (2002).
- [13] A. Bourdier, Phys. Fluids **26**, 1804 (1983); P. Gibbon and A. R. Bell, Phys. Rev. Lett. **68**, 1535 (1992).
- [14] W. L. Kruer and K. G. Estabrook, Phys. Fluids **28**, 430 (1985).
- [15] S. Kato *et al.*, *Proc. of the Seventh International Symposium of the Graduate University for Advanced Studies on Science of Super-Strong Field Interactions, Hayama, JAPAN, 2002*, Editors: K. Nakajima and M. Deguchi, p.290 (American Institute of Physics, 2002) .
- [16] Wei Yu *et al.*, Phys. Rev. Lett. **85**, 570 (2000); T. E. Cowan *et al.*, Phys. Rev. Lett. **84**, 903 (2000).

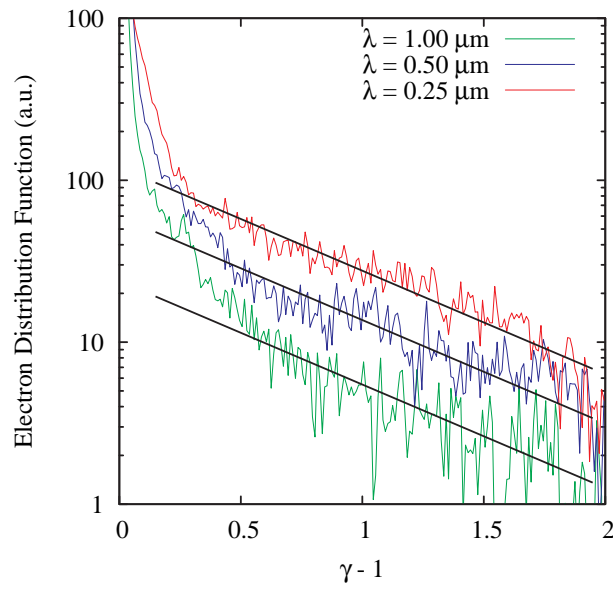
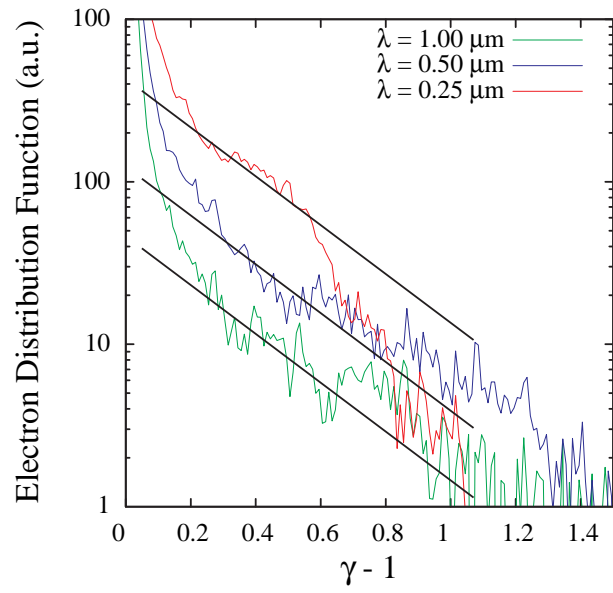


Figure 1. Electron energy distribution at $t = 50$ fs and $I = 5 \times 10^{19}$ W/cm² for (a) $\theta = 30^\circ$ and (b) $\theta = 45^\circ$, respectively. The red, blue, and green lines are for $\lambda = 0.25$, 0.5 , and $1 \mu\text{m}$, respectively.